

# CHAPTER - 7

## MICROHARDNESS OF $\text{In}_x\text{Bi}_{2-x}\text{Te}_3$ CRYSTAL

## CHAPTER – 7

### Microhardness of $\text{In}_x\text{Bi}_{2-x}\text{Te}_3$ Crystal

This chapter reports the results obtained in the microhardness studies on  $\text{In}_x\text{Bi}_{2-x}\text{Te}_3$  with ( $x = 0.1$  to  $0.5$ ) single crystals. The Vickers diamond pyramidal indenter was used for the microhardness indentation tests on the cleavage plane (0001) of the crystal. Part – A deals with the variation of hardness with applied load and its temperature dependence. Part – B deals with the study of indentation hardness creep.

#### Part – A

The indentation method is most efficient and widely used method for measurement of hardness of metallic and non-metallic crystals. This is because it does not require large specimens and even on a small specimen a number of measurements can be made. The Vickers indenter has the included angle  $136^\circ$  gives a well defined geometrical square shaped indentation mark. Also during the diamond contact with the cleavage surface of a metal, the coefficient of friction ranges from 0.1 to 0.15 making the frictional effect less pronounced [1]. The Vickers hardness is defined as the ratio of applied load to the pyramidal contact area of indentation and it is calculated as

$$H_v = \frac{1854 \times P}{d^2} \text{ (Kg/mm}^2\text{)} \text{ ----- (1)}$$

where,  $H_v$  = Vickers microhardness in  $\text{kg/mm}^2$   
 $P$  = Applied load in gm  
 $d$  = Mean diagonal length of the indentation mark in  $\mu\text{m}$ .

The nature of variation of hardness with load is quite complex and does not follow any universal rule and a large number of workers have studied the load dependence of hardness. For example, the load dependence of hardness was observed by Bergsman [2]. Rostoker [3] studied the load variation of hardness in the case of copper and concluded that there is remarkable decrease in hardness at low applied loads. Grodzinsky [4] found that plot of hardness versus load shows a peak at low applied loads. Whereas Taylor [5] and Toman et al [6] have reported no significant change in hardness value with variation of load. These contradictory reports [2-6] may be due to the effect of surface layers and other adverse experimental conditions like vibrations produced during the indentation.

Because of these different observations and conclusions as described above, by various previous workers, it can be said that establishing any definite relationship between microhardness and applied load is a difficult task. This is because equation (1) indicates the hardness to be independent of load and the applied load 'P' should be directly proportional to square of the diagonal 'd'

$$P = ad^2 \text{ -----(2)}$$

where a is the material constant. This equation is known as Kick's law. Then

the observed hardness dependence on load implies that the power index in this equation should differ from 2 and according to Hanemann [7], the general form of dependence of load on the diagonal length should be

$$P = ad^n \text{ -----(3)}$$

(Mayer's law) where the dependence of hardness on load reflects in the deviation of the value of the index 'n' from 2. Thus, the variation of microhardness with applied load is a controversial issue.

In the present work on  $\text{In}_x\text{Bi}_{2-x}\text{Te}_3$  single crystals, the dependence of hardness on load, In concentration, temperature, cold working, annealing and loading time was studied. Single crystals grown at the growth speed of 0.4 cm/hr. by zone melting method obtained after 10 passes were used for the microhardness study and the results are presented below.

To decide the indentation time to be kept constant during the hardness measurements at room temperature, experiments were performed for various indentation times from 5 seconds to 60 seconds keeping applied load constant at 50gms, which is sufficiently a high load at which the hardness was observed to be insensitive to small load variations. Figure-1 shows the plot of  $H_v$  versus  $t$  for  $\text{In}_{0.1}\text{Bi}_{1.8}\text{Te}_3$  as an example. For this plot it can be seen that hardness is high for small indentation times. As the indentation time increases, the hardness decreases and tends to become constant for indentation time 20 seconds or more. Hence the indentation time of 20 second was kept constant to study other hardness variations.

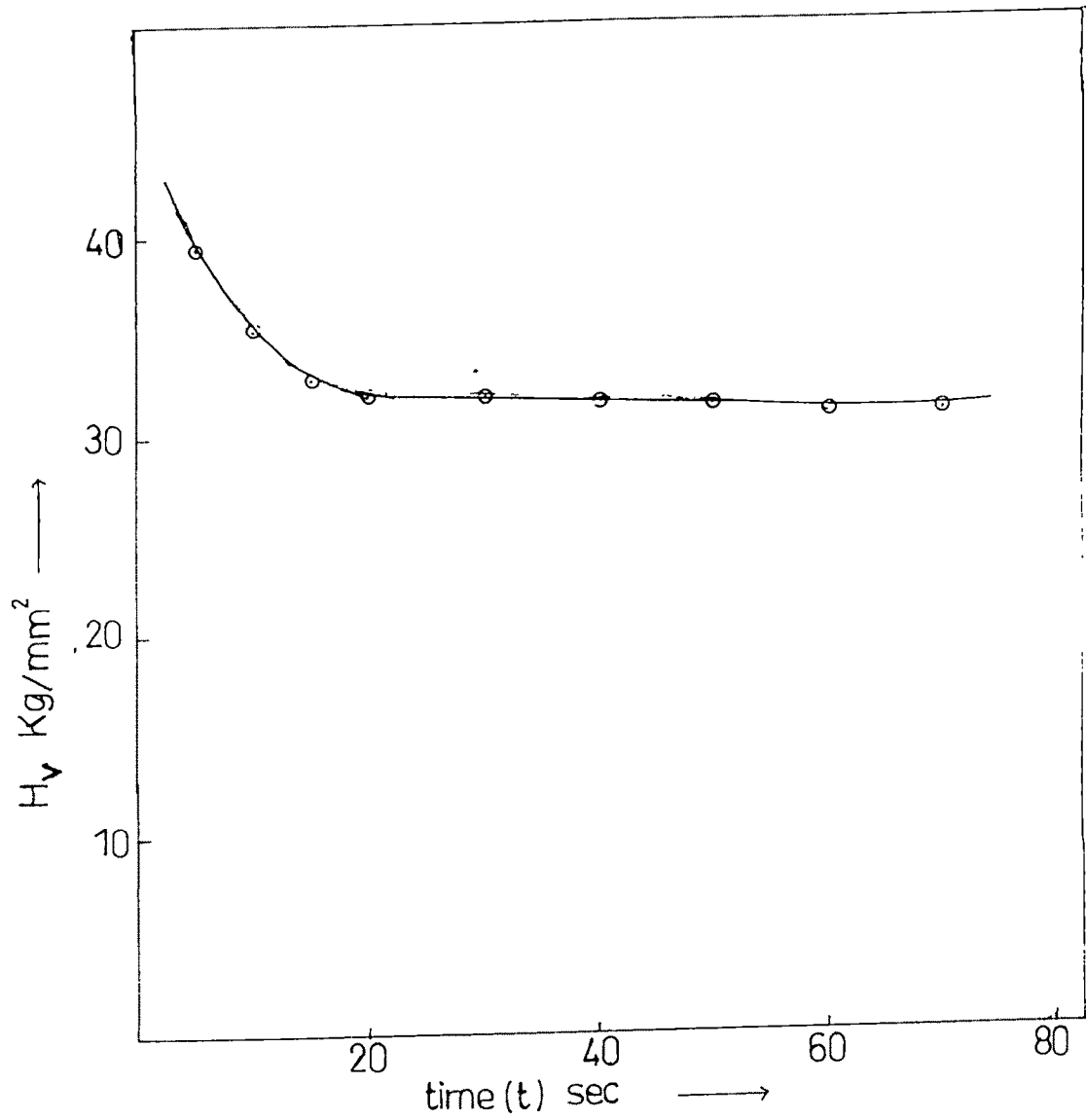


Fig.1. Plot of  $H_v$  versus time (t).

### **Variation of hardness with Load :**

The hardness indentations were made under different loads from 5 gms to 80gms. Loads less than 5 gms were also tried but the indentation mark obtained was too small in size causing large errors in measurement. On the other hand, loads greater than 90 gms also could not be used since the size of the indentation marks obtained at higher loads exceeded the maximum range of measurement in the micrometer eyepiece. However, the range of load used includes the essential part of interest in the microhardness region. The shape of the indentation mark produced is square irrespective of the relative azimuthal orientation of the surface and the indenter. Fig 2 shows a typical indentation mark obtained under 20 gms. It can be seen that the indentation mark is nearly perfect square with all sides equal and about equal length of the two diagonals. At least three indentations were produced at each applied load and they were repeated on three samples. The results present average of the hardness values obtained. All necessary precautions were taken to see that the experimental error in the indentation and measurement are as small as possible.

Fig.3 shows the plots of Vickers hardness ( $H_v$ ) versus applied load (P) for different indium concentrations in  $\text{Bi}_2\text{Te}_3$ . The graph displays three distinguishable regions. In the low load region the hardness has complex load dependence and it can be explained in terms of the depth of penetration of the indenter and consequent strain hardening of the surface layers. Now the depth



X 600

FIG.2

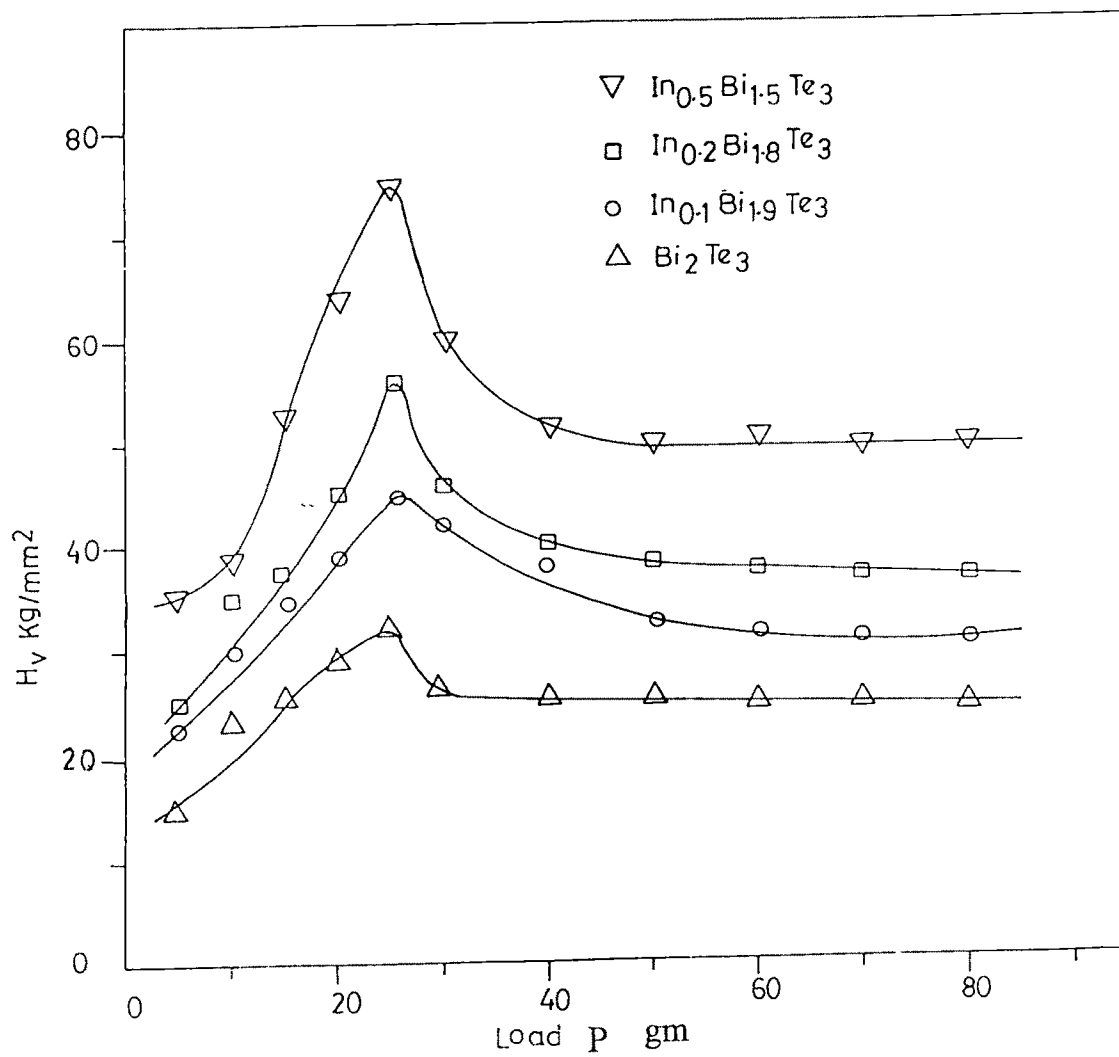


Fig.3. Plots of hardness ( $H_v$ ) versus load (P).

of penetration depends usually on three factors :

- (1) The type of surface receiving the load which can again be divided into three categories :
  - (a) Surface layer having different degree of cold working [7],
  - (b) Surface layer having finely precipitated particles [8],
  - (c) Surface layer having different grain size [9] and number of grains indented [10], if the specimen is a polycrystal.
- (2) The magnitude of the applied load and
- (3) Accuracy in the normal operation of indenting the specimen and the rate at which the indentation is carried out, i.e. the strain rate. The time taken to realize the full load will evidently decide the strain rate.

All these factors play a prominent role when hardness tests are carried out by indentation at low load. The surface layer-sensitive initial increase in hardness with load can be explained in terms of strain hardening based on dislocation theory. It is known that dislocations are surrounded by elastic stress fields. The stress fields of different dislocations interact strongly and lock the dislocations into metastable configurations. The effect becomes quite pronounced in metals and semimetals where the dislocation mobility is usually high. Individual dislocations move readily at much lower stresses. The flow that occurs during indentation is therefore not limited by drag on isolated

dislocations. The interactions between dislocations create jogs on them and these jogs create trails of dislocation dipoles behind the moving dislocations. As the penetration proceeds, the structure soon becomes filled with interacting dislocations forming complex networks resulting into efficient barriers to the motion of new dislocations. Further flow is then limited by the strength of interaction between the barriers and dislocations. The externally applied stress required to produce further plastic deformation must be sufficient to make the dislocation move through the opposing stress fields of these interactions. The effective dislocated zones in the damaged layer causing such back stresses have been termed as “coherent regions”. [11,12]. The coherent region in the present case extends to the depth of penetration of the indenter produced by the load at the hardness peak, i.e. about 25  $\mu\text{m}$ . For  $\text{In}_x\text{Bi}_{2-x}\text{Te}_3$ , in the higher load range the hardness tends to be independent of applied load, particularly at loads higher than 50  $\mu\text{m}$ . In this respect, the average hardness obtained may safely be taken to represent the hardness of the bulk, since at the higher loads the penetration depth of the indenter is well beyond the surface layers. Hence the hardness sensed is that of the interior bulk of the sample, the effect of surface layers being none or negligible. Accordingly the hardness values of  $\text{Bi}_{2-x}\text{In}_x\text{Te}_3$  single crystals with  $x = 0$  to 0.5 are as shown in

Table-1. Fig.4 shows the plot of hardness versus indium concentration in  $\text{Bi}_2\text{Te}_3$ . It is seen that the hardness increases with indium concentration. It is interesting to find that this increase is nearly linear with indium concentration.

In this respect it should be noted that indium forms an equilibrium phase with Te, namely,  $\text{In}_2\text{Te}_3$ . In the present crystal the XRD data indicate presence of this phase in the material (Chap.-6 growth)  $\text{In}_2\text{Te}_3$  has a band gap of about 1.0 eV which is quite higher than that of  $\text{Bi}_2\text{Te}_3$ , and is dominated by stronger co-valent bonds. Hence with increasing indium in  $\text{Bi}_2\text{Te}_3$ , the increase in hardness is expected. It is customary to analyze the indentation marks in terms of Mayer's law,  $P = ad^n$  where P is the applied load, d is the diagonal length of the indentation mark and a and n are constants of the material. This is because the constant n, known as Mayer index equals 2 for load independent hardness. The variation of n reflects the dependence of hardness on load [13]. Using the data obtained of the diagonal length 'd' for different applied loads P, the plots of  $\ln P$  and  $\ln d$  were obtained (Fig.5) and n was calculated for all indium concentrations. There are two distinct regions obtained. The value of  $n_1$  and  $n_2$  of the two straight lines making up each plot are listed in Table-2, for all impurity concentrations. A careful study of these data would indicate that the

**Table -1**

x of In in $\text{In}_x\text{Bi}_{2-x}\text{Te}_3$	Constant hardness $\text{kg/mm}^2$
0	25.0
0.1	30.6
0.2	36.2
0.5	50.0

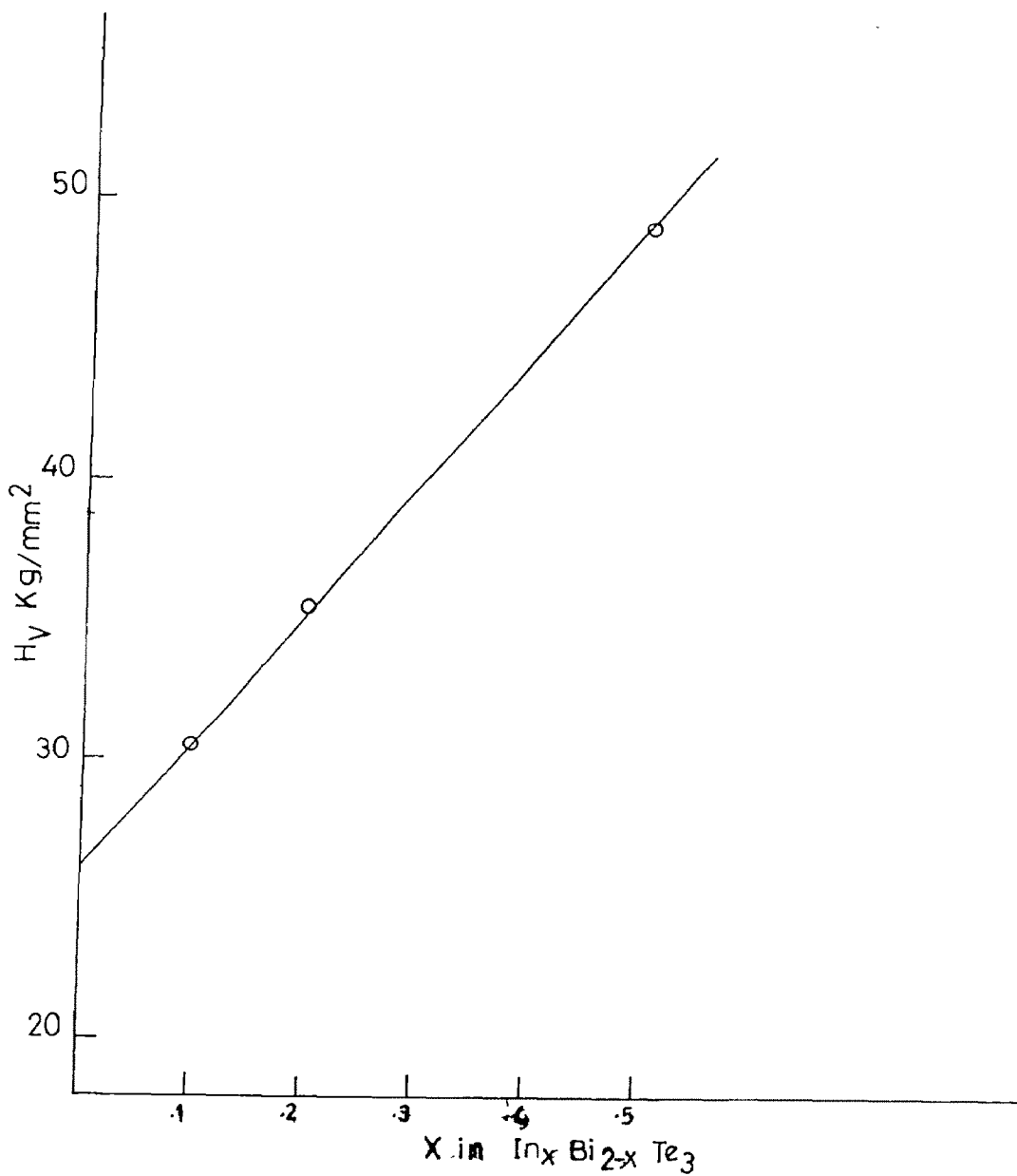


Fig.4. Plot of Constant hardness ( $H_v$ ) versus x in  $\text{In}_x\text{Bi}_{2-x}\text{Te}_3$ .

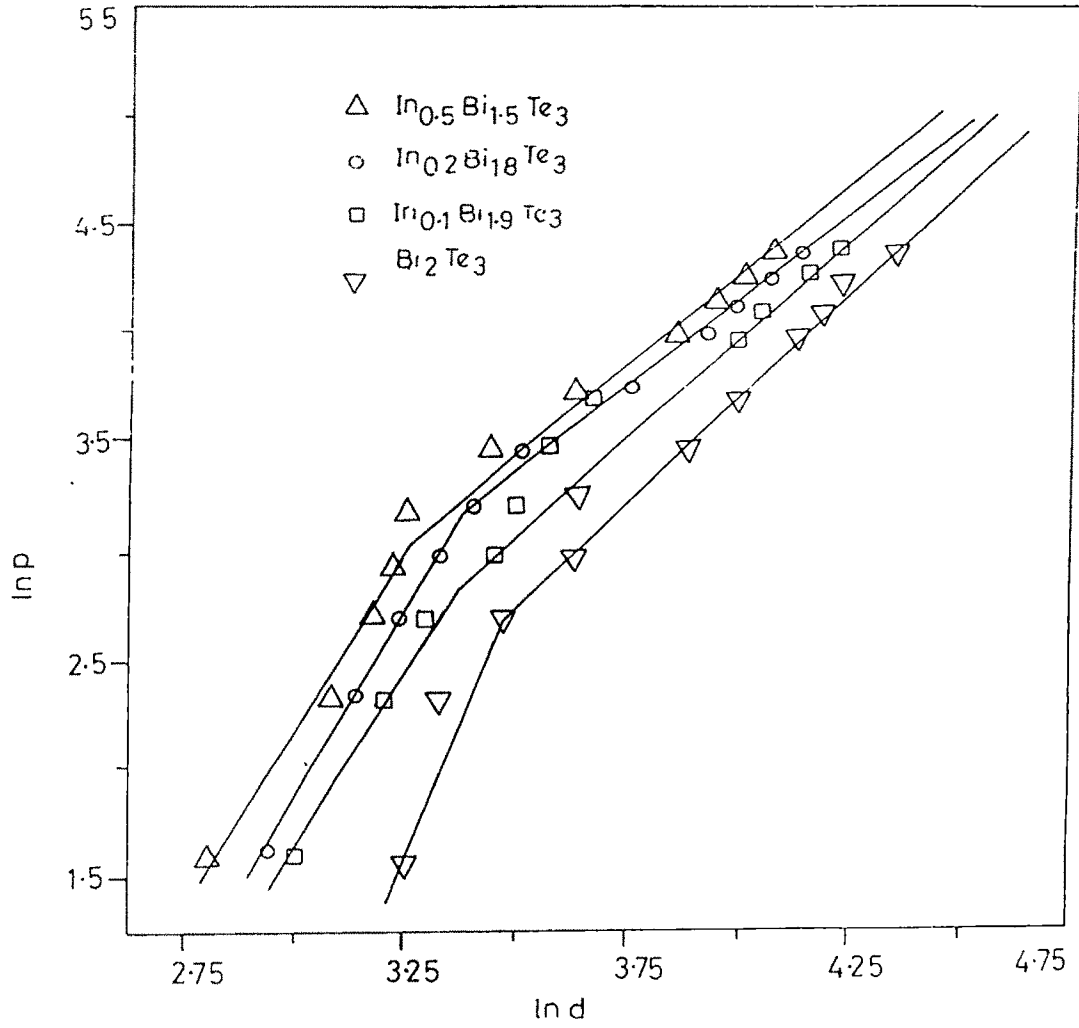


Fig.5. Plots of  $\ln P$  versus  $\ln d$ .

**Table-2**

x of In in $\overline{\text{In}_x\text{Bi}_{2-x}\text{Te}_3}$	$n_1$	$n_2$
0	5.60	2.08
0.1	3.08	1.93
0.2	4.00	1.98
0.5	3.23	1.92

exponent  $n_1$  is greater than 2.0 in LLR. In the LLR a few surface layers are penetrated by the indenter and the measured hardness is only a characteristic of these layers, the fact responsible for the work hardening with the progressing penetration and hence the observed deviation of  $n_1$  from 2. The value of  $n_2$  deviates maximum by about 10% from its standard value 2, whereas  $n_1$  deviates by as much as 140% indicating highly load sensitive hardness for all impurity concentration in LLR.  $n_2 \approx 2$  for all concentration implies nearly load independent hardness in the HLR.

#### **EFFECT OF COLD WORKING :**

To study effect of work hardening on the load dependence of hardness in the LLR, the crystals ( $\text{In}_{0.5}\text{Bi}_{1.5}\text{Te}_3$ ) were cold worked prior to indentation. For this purpose 5 to 6mm thick cleaved plates of the crystals were placed between two flat glass slabs and a load of about 2 Kg was placed over the top slab. This effectively produced compression along the c-axis of the crystals. The compression was continued for 24 hrs. The experiments were conducted at room temperature. Then the crystals were cleaved to obtain 1 to 2 mm thick slices and the Vickers indentations were carried out at different loads. The experiment was conducted on a number of samples with similar treatment.

Fig.6 shows average results of dependence of hardness  $H_v$  on applied load  $P$  for all the three cold worked crystals. It is interesting to compare these plots

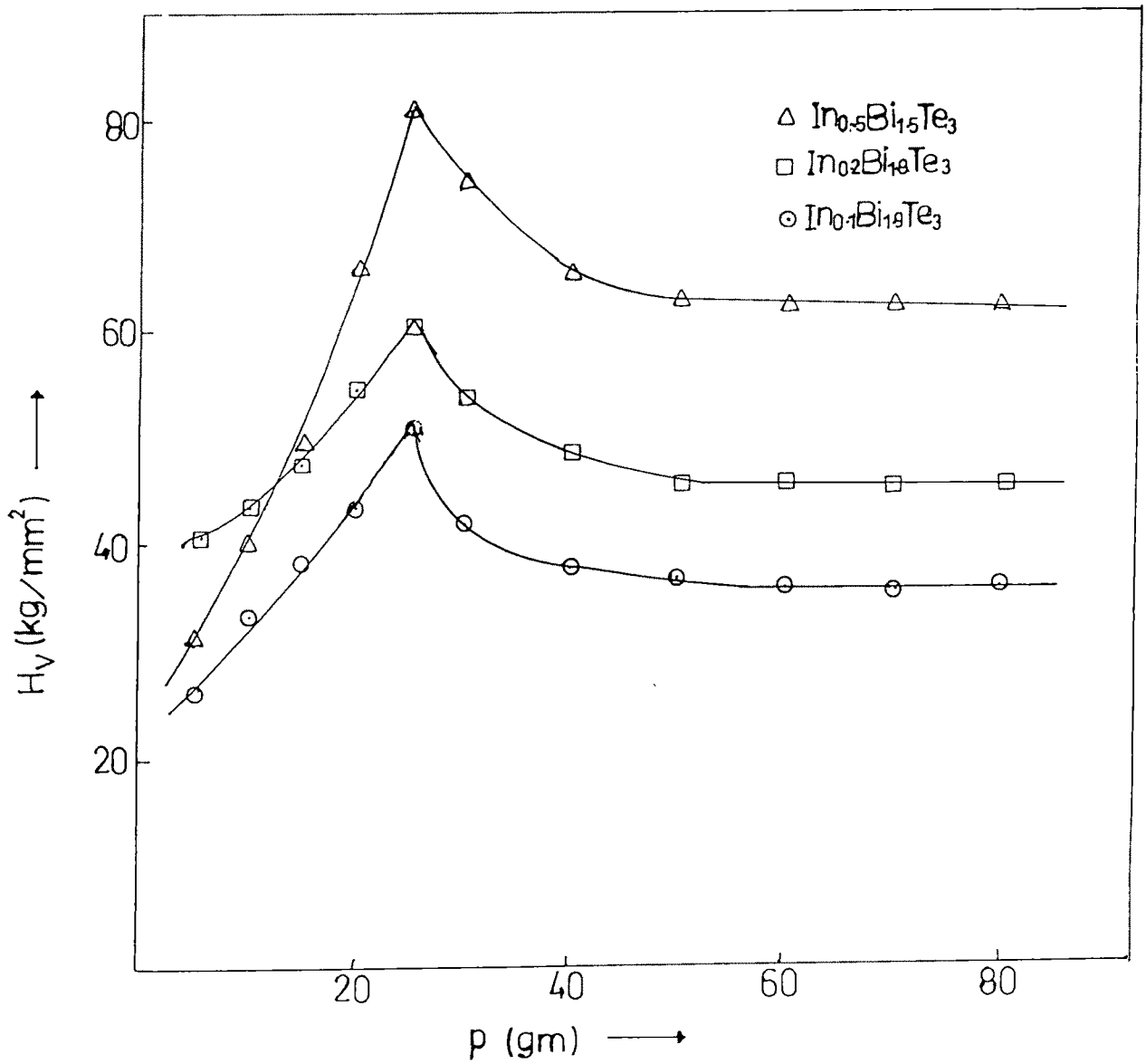


Fig.6. Plots of hardness ( $H_v$ ) versus load (P) for cold worked crystals.

with corresponding plots in Fig.3. It is seen that the peak hardness value increases in the case of the cold worked samples as compared to those obtained in the case of untreated crystals. This fact probably indicates that the extent of coherent region below the surface gets limited by the work hardening. In other words, due to cold working, the overall dislocation network increases in strength and number and produces barrier to generation and motion of new dislocation in the vicinity of the surface. Likewise the saturation hardness, i.e., the load independent hardness has also increased to a considerable extent. It has increased from 30 kg/mm<sup>2</sup> to 36 kg/mm<sup>2</sup>, 36 kg/mm<sup>2</sup> to 45 kg/mm<sup>2</sup> and 50 kg/mm<sup>2</sup> to 62 kg/mm<sup>2</sup> for In<sub>0.1</sub>Bi<sub>1.9</sub>Te<sub>3</sub>, In<sub>0.2</sub>Bi<sub>1.8</sub>Te<sub>3</sub> and In<sub>0.5</sub>Bi<sub>1.5</sub>Te<sub>3</sub> crystals, respectively. Thus the work hardening effect is to an extent of 20%, 22% and 24% respectively for the three crystals, showing an increasing trend with the indium content.

#### **Effect of Annealing on Hardness :**

For annealing study, the sample was sealed in a quartz ampoule at 10<sup>-4</sup> Pa. It was kept in the furnace at 375°C for about 48 hrs. and gradually cooled down to room temperature. The hardness tests were then carried out on the cleavage surfaces of the annealed crystals.

Fig.7 shows the plots of H<sub>v</sub> versus load (P) obtained for the In<sub>x</sub>Bi<sub>2-x</sub>Te<sub>3</sub> with x = 0.1 to 0.5 crystals. In the low load range the hardness remains dependent on load while at higher loads it remains practically independent of load. The

hardness values of  $\text{In}_{0.1}\text{Bi}_{1.9}\text{Te}_3$ ,  $\text{In}_{0.2}\text{Bi}_{1.8}\text{Te}_3$  and  $\text{In}_{0.5}\text{Bi}_{1.5}\text{Te}_3$  crystals obtained in these plots are 27, 32 and 41  $\text{kg/mm}^2$  respectively. Compared to the values of as-grown crystals, the hardness values of these crystals have reduced to an extent of 10% 14% and 20%, respectively. It is observed that softening of crystal takes place and the hardness decreases to a considerable extent as a result of annealing. Annealing is known to decrease dislocation density and to free immobile dislocation tangles, thus causing the plastic softening of the crystals. This trend indicates the crystal with highest In content to be capable of maximum work hardening and maximum anneal softening. Since these phenomena are largely dependent on dislocation mobility the comparative results of cold-working and annealing would therefore indicate high dislocation mobility in  $\text{In}_{0.5}\text{Bi}_{1.5}\text{Te}_3$  crystals.

#### **Effect of Anisotropy on Crystals :**

In order to study anisotropy exhibited by (0001) plane of the crystals, the directional hardness was determined by producing indentation at various azimuthal orientations of the indenter with respect to the surface over a range 0-180°. The crystal was rotated about the indenter axis in steps of 15° while keeping the applied load and loading time constant at 50gm and 20 sec, respectively.

The surface anisotropy of  $H_v$  in the  $\text{In}_{0.1}\text{Bi}_{1.9}\text{Te}_3$ ,  $\text{In}_{0.2}\text{Bi}_{1.8}\text{Te}_3$  and  $\text{In}_{0.5}\text{Bi}_{1.5}\text{Te}_3$  crystals are presented in Fig.8 in the form of plots of  $H_v$  versus orientation

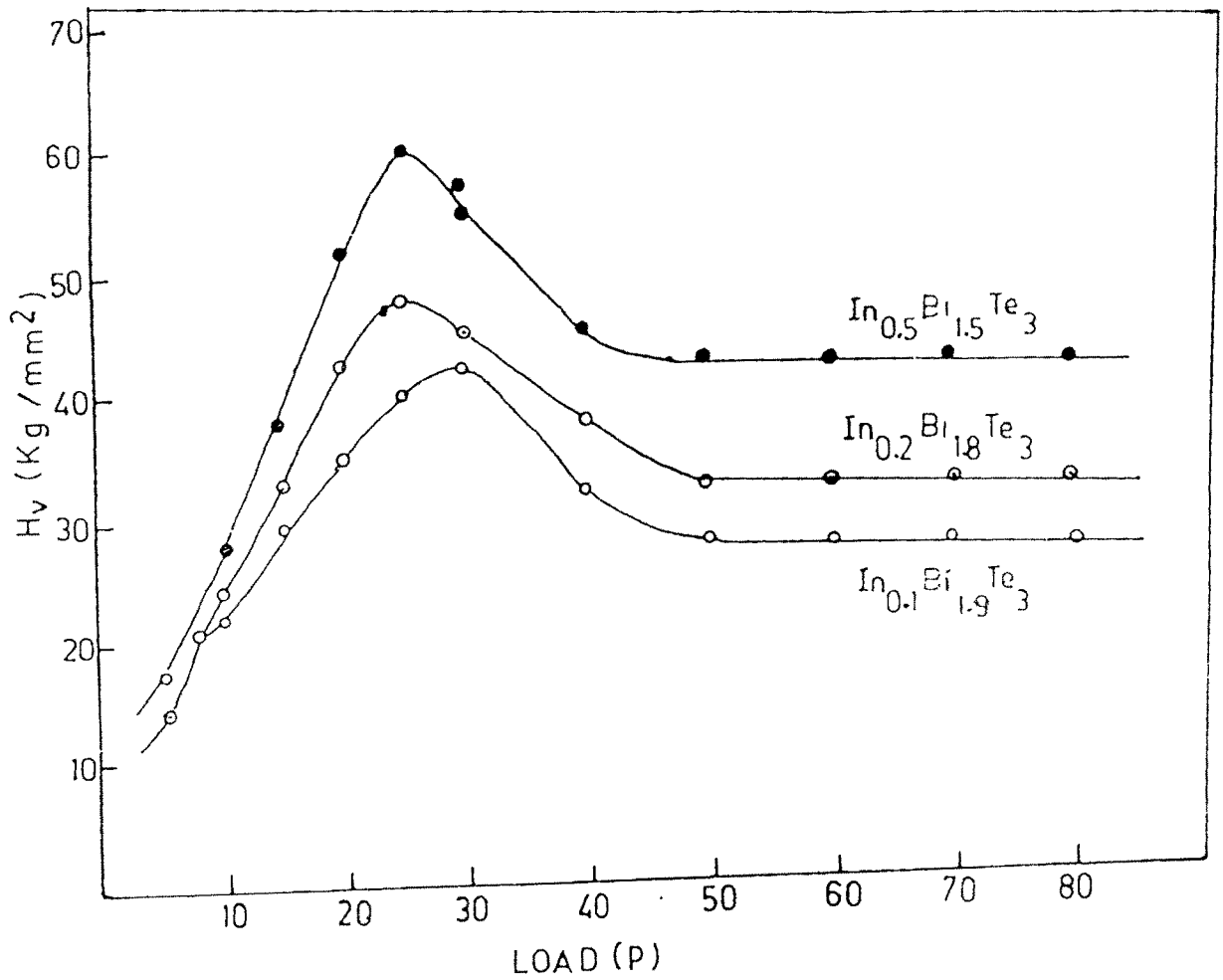


Fig.7. Plots of hardness ( $H_v$ ) versus load ( $P$ ) for annealed crystals.

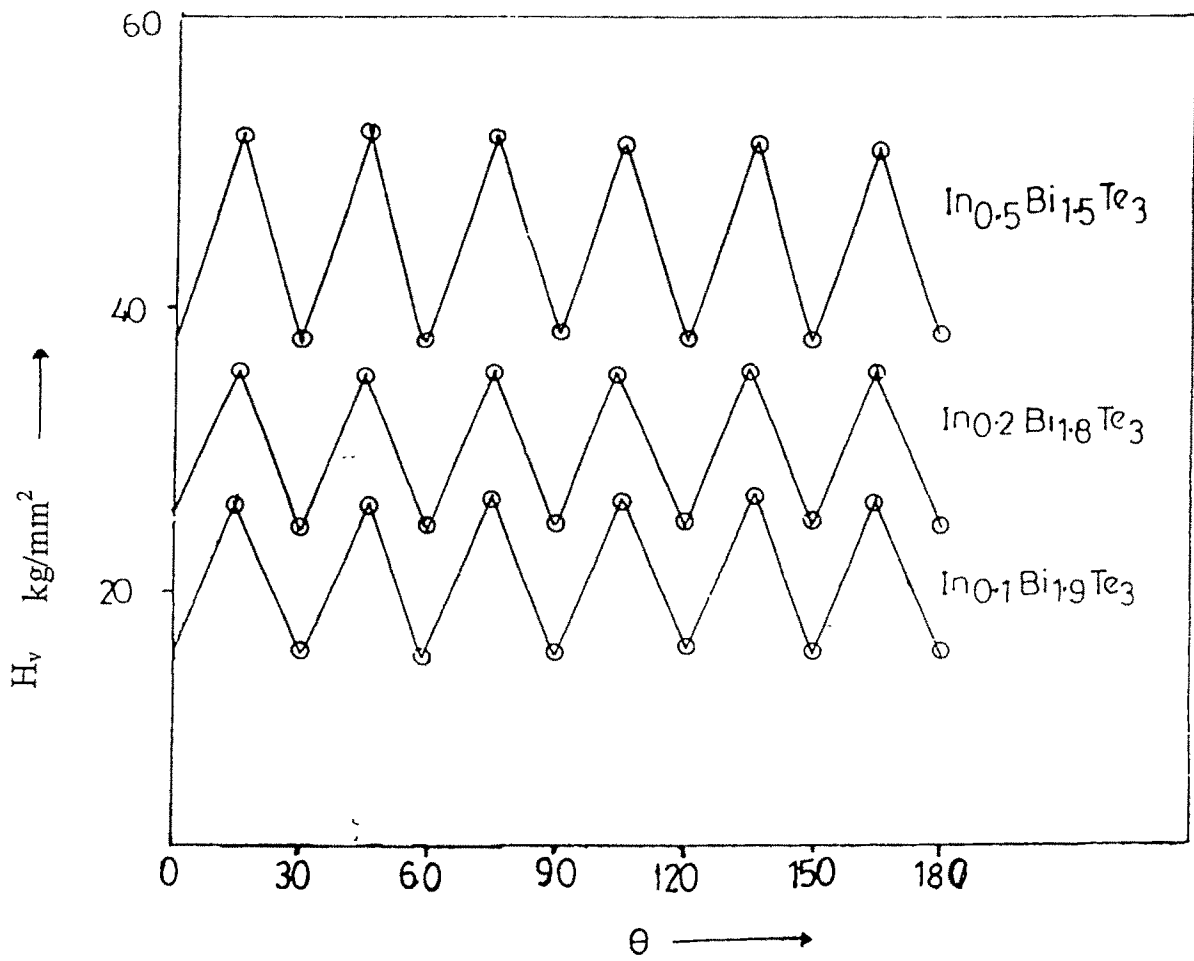


Fig.8. Plots of hardness ( $H_v$ ) versus orientation angle ( $\theta$ )

angle,  $\theta$ . As can be seen there are periodic variations of  $H_v$  with  $\theta$ . The maxima (minima) repeat at every  $30^\circ$  interval in all the three cases. Thus the hardness exhibits twelve fold rotation symmetry on the cleavage planes of the crystals. This is a result of the four fold symmetry of the indenter combined with the six fold symmetry of the crystals. Further, for  $\text{In}_{0.1}\text{Bi}_{1.9}\text{Te}_3$  the value of maximum and minimum hardnesses are  $30 \text{ kg/mm}^2$  and  $18 \text{ kg/mm}^2$ ; for  $\text{In}_{0.2}\text{Bi}_{1.8}\text{Te}_3$ , they are  $35 \text{ kg/mm}^2$  and  $29 \text{ kg/mm}^2$ , for  $\text{In}_{0.5}\text{Bi}_{1.5}\text{Te}_3$   $50 \text{ kg/mm}^2$  and  $38 \text{ kg/mm}^2$ , respectively. Thus there are anisotropic variations to the extent of 17% to 40%.

## PART – B

### Creep and Activation energy of Flow Process :

This part reports the results obtained in the study of variation of microhardness with time at different temperatures of single crystals of  $\text{In}_{0.1}\text{Bi}_{1.9}\text{Te}_3$ ,  $\text{In}_{0.2}\text{Bi}_{1.8}\text{Te}_3$ , and  $\text{In}_{0.5}\text{Bi}_{1.5}\text{Te}_3$ . The Vickers microhardness indentation tests were carried out on the cleavage surface of the crystals using a constant load and varying the time of indentation. The results obtained have been used to determine the activation energy for creep.

In assessing the strength of a crystal the indentation method assumes the hardness of a crystal to be independent of time after the load is fully applied. In fact, the indenter generally sinks into the crystal surface even after the application of full load. This is known as indentation creep. The use of

indentation hardness is well known for the study of plastic yield of solids. The general behaviour regarding the decrease in the hardness with increasing loading time may be described by an empirical formula given by Atkins et al [14] and which incorporates the earlier relations given by the previous workers [15-17]. The behaviour of hardness closely parallels the creep characteristics of materials in unidirectional stress tests. Using a transient creep equation derived by Mott.[18] for constant stress conditions and assuming that it can be applied even when the stress changes, Atkins et al [14] analyzed the kinematics of creep process during indentation. They obtained good agreement between theory and experiment. Activation energy derived from the hardness measurements were close to the activation energies for self-diffusion. Their analysis suggested that in spite of its limited validity, a transient-creep equation of state may be used to describe the hardness behaviour of solids at elevated temperatures.

The time dependence of plastic deformation [i.e.creep] plays a prominent role in hardness measurements. The nature and amount of plastic deformation and measured hardness depend on temperature.

Recently in 1992, Fujiwara et al[19] have studied the indentation creep in tin crystals which deform by pencil glide. The investigation was on the deformation mechanism of (001) pencil glide in the crystals at temperatures 298K, 333K and 373K. The steady state deformation due to pencil glide is rate

controlled probably by cross slip between planes containing the (001) slip vector. Plastic deformation of single crystals of pure InP oriented for single glide has been studied in compression creep at 1068K and under a load of 9 MPa [20]. A. Ayenus et al [21] have studied the power law creep of wire specimens tested at temperatures 573K, 673K and 773K under different uniaxial stresses. The values of the stress exponent and activation energies indicated the rate controlling mechanism for creep to be associated with grain boundary. In any case, a successful hardness time relation in terms of temperature and creep activation energy as given by Alkins et al [14] can be used.

In this laboratory different workers have studied the time dependence of microhardness on different crystals [22-26].

In view of the above, it was thought worthwhile to undertake the study of indentation creep of  $\text{In}_x\text{Bi}_{2-x}\text{Te}_3$  with  $x = 0.1, 0.2$  and  $0.5$  single crystals.

For the analysis of the data the well established Atkins relation was used:

$$H_{vo}^{-3} - H_o^{-3} = A \exp \left[ \frac{-Q}{3RT} \right] (t^{1/3} - t_o^{1/3}) \text{-----(4)}$$

where,

- $H_{v_0}$  = The hardness value at time  $t_0$
- $H_0$  = The hardness value immediately after attaining the full load  
P at time  $t_0$
- $t$  = time
- $Q$  = Activation energy for creep
- $R$  = The gas constant
- $A$  = Constant
- $T$  = Absolute temperature

This simplified equation has been used to determine the activation energy for creep. The equation can be written in a convenient form as

$$\ln (H_v^{-3} - H_{v_0}^{-3}) = \ln A + \ln (t^{1/3} - t_0^{1/3}) - \frac{Q}{3RT} \quad \text{-----(5)}$$

All the observations were obtained on freshly cleaved basal faces of these crystals, using Vickers pyramidal indenter. As discussed before microhardness has a complex load dependence for small applied loads. The zero load condition was assured to give a maximum load error to be 0.200 gm and a load of 50 gm was selected to minimize microhardness variation due to error in applied load. Data obtained for different indentation times at different temperatures have been used for the creep study on three sample of each

composition. The indentations of the specimen were carried out at 303K, 323K, 353K and 373K and the indentation time was varied from 5 sec. to 60 sec. at each temperature. The temperature could not be exceeded beyond 380K since there was no provision of heat shield for the hardness tester to prevent possible damage of indenter objective at higher temperatures.

It has been observed that when all parameters are kept constant, the microhardness decreases with increasing temperature. Fig 9,10,11 show the plots of  $\ln H_v$  versus  $T / T_m$  where  $H_v$  is the Vickers hardness and  $T$  and  $T_m$ , the indentation temperature and melting point, respectively, both in Kelvin. It can be seen that the plot is straight line with negative slope indicating a fast decrease in  $H_v$  with increase of temperature in agreement with hardness temperature relationship [14,15].

$$H = A \exp (-BT) \text{ ----- (6)}$$

where the constant  $B$  is known as softening parameter of the crystal and  $A$ , the extrapolated intrinsic hardness. Similar decrease in hardness was found in the case of Si, Ge and Cu crystals [16]. From the graphs, softening parameter  $B$  is found to be  $\sim 78.6 \times 10^{-4} \text{ K}^{-1}$ , for  $\text{In}_{0.2}\text{Bi}_{1.8}\text{Te}_3$  crystal. Similar nature was observed for the other two crystals, and the values of softening parameter were found out to be  $86.7 \times 10^{-4} \text{ K}^{-1}$  and  $59.1 \times 10^{-4} \text{ K}^{-1}$  for  $\text{In}_{0.1}\text{Bi}_{1.9}\text{Te}_3$  and  $\text{In}_{0.5}\text{Bi}_{1.5}\text{Te}_3$  crystals.

The plot of  $\ln H_v$  versus  $\ln t$  obtained at different temperatures are shown in

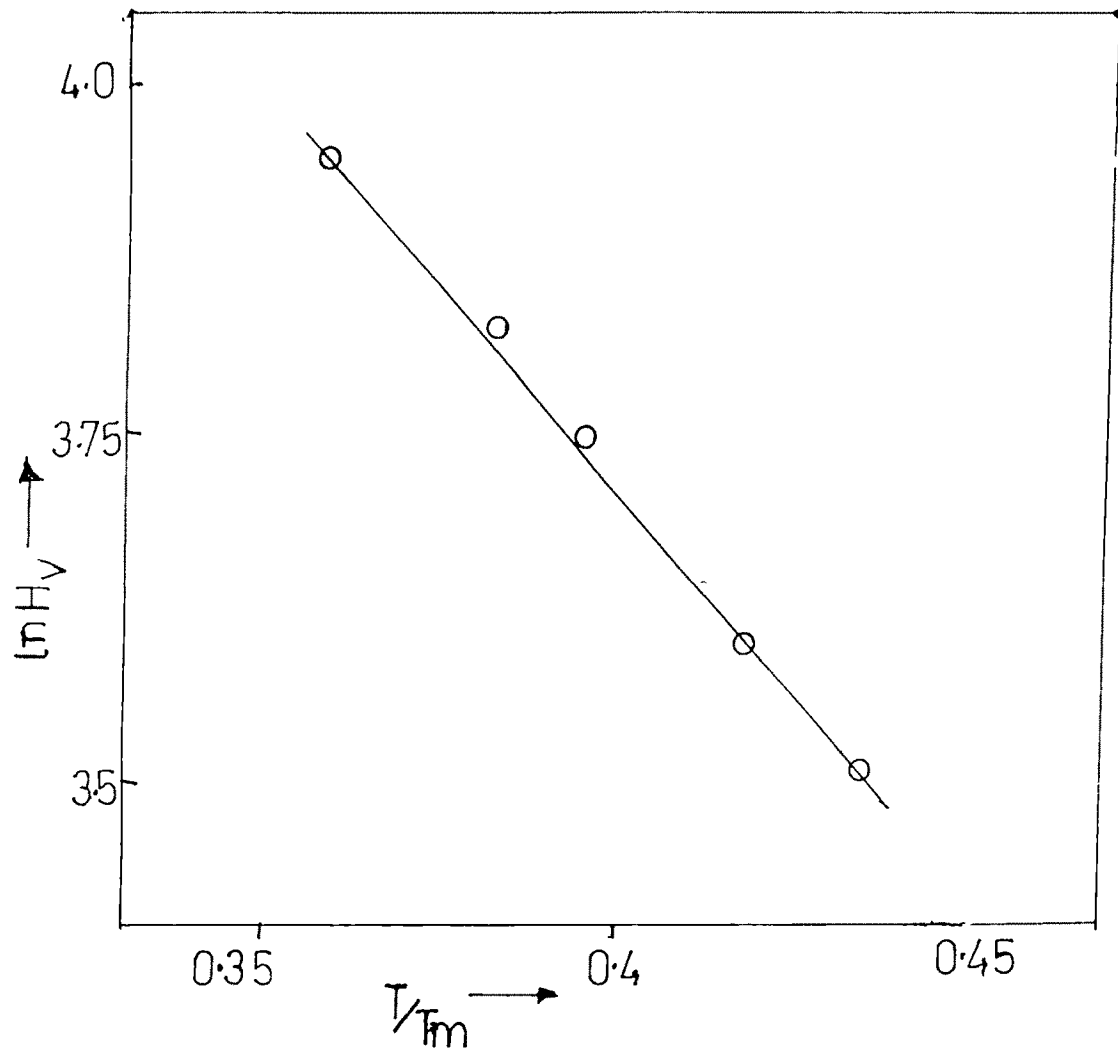


Fig.9. Plots of  $\ln H_v$  versus  $T/T_m$  for  $\text{In}_{0.1}\text{Bi}_{1.9}\text{Te}_3$  crystals.

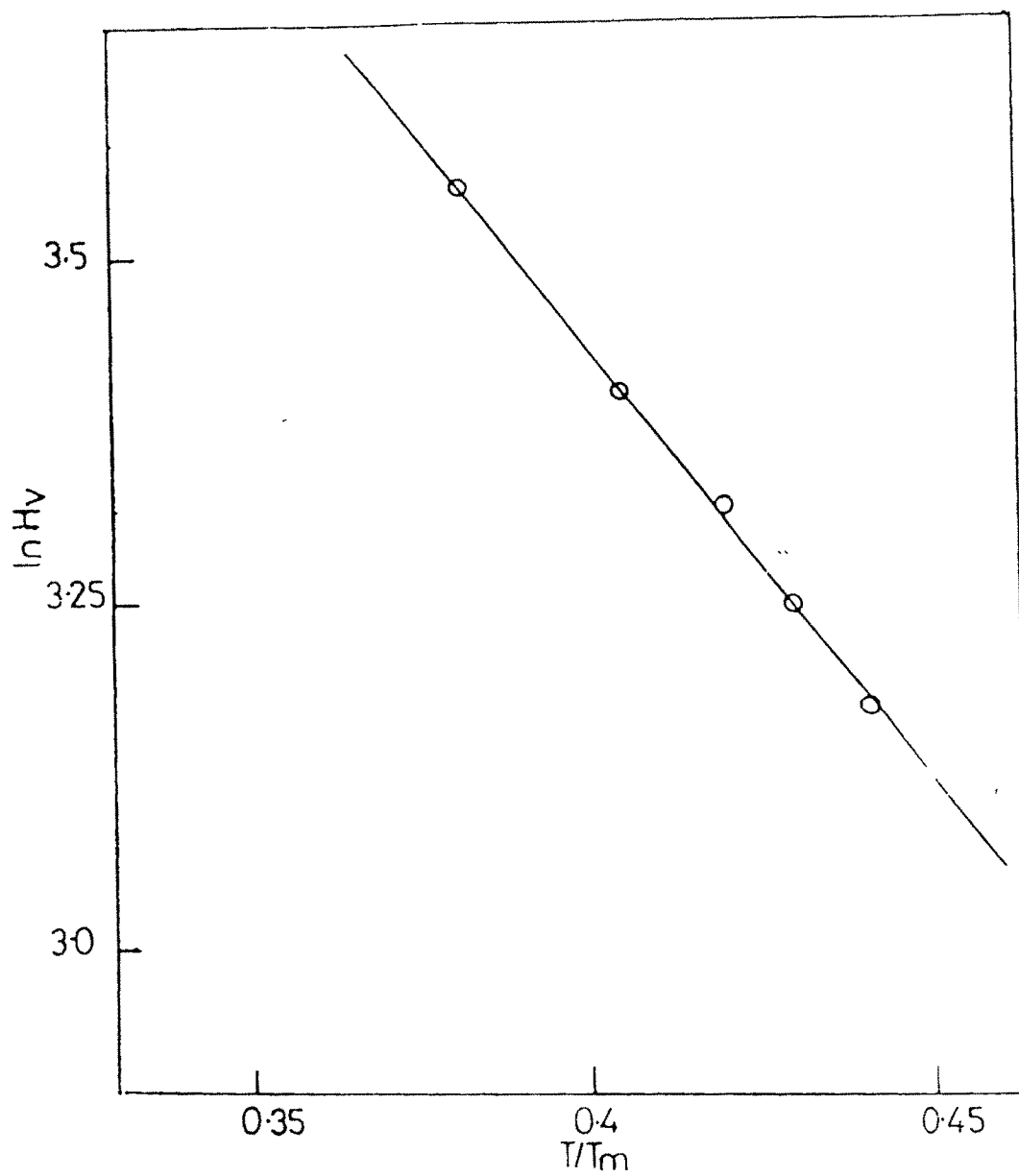


Fig.10. Plots of  $\ln H_v$  versus  $T/T_m$  for  $\text{In}_{0.2}\text{Bi}_{1.8}\text{Te}_3$  crystals.

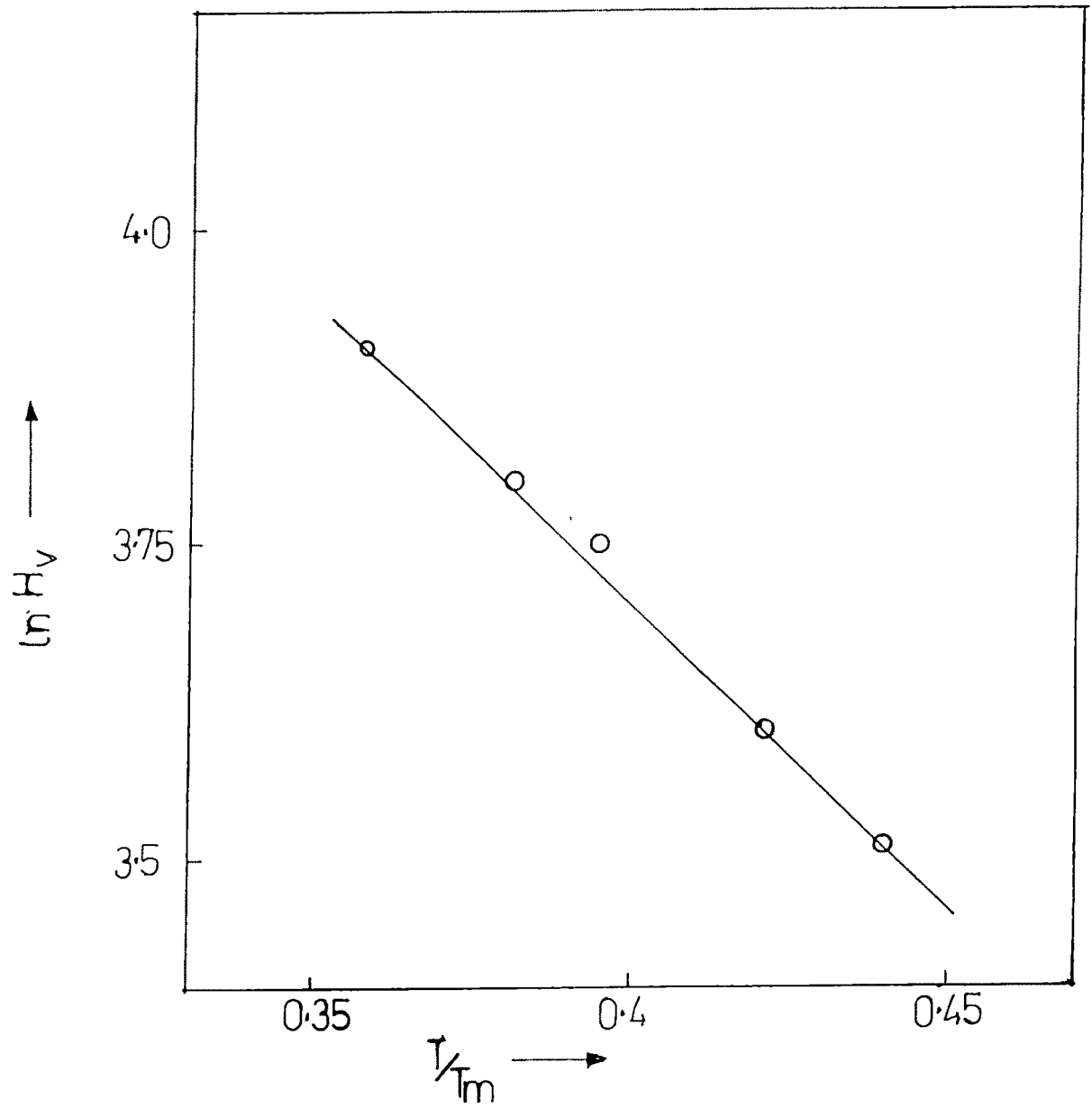


Fig.11. Plots of  $\ln H_v$  versus  $T/T_m$  for  $\text{In}_{0.5}\text{Bi}_{1.5}\text{Te}_3$  crystals.

Fig.12,13,14. It can be seen that  $\ln H_v$  varies linearly with  $\ln t$  and the slope of the straight line increases with temperature as predicted by Atkins et al[14]. For each temperature,  $H_{v0}$  was obtained for  $t_0 = 1$  sec from the plots in Figure 12,13,14. Figure 15,16,17 show plots of  $\ln (H_v^{-3} - H_{v0}^{-3})$  versus  $\ln (t^{1/3} - t_0^{1/3})$  at different temperatures. These are straight lines, all of almost equal slopes close to unity, in accordance with equation (5).

To evaluate  $Q$  the usual method is to find difference between intercepts at two temperatures  $T_1$  and  $T_2$  in these graphs. (Fig. 15,16,17) and to equate it to

$$Q/3R (1/T_1 - 1/T_2)$$

under the assumption that  $Q$  remains constant with temperature. However, in many cases  $Q$  has been found to be different in different temperature ranges. Hence an alternative method which does not assume  $Q$  to be constant with temperature has been used. From the plots of Fig. 15,16,17 three sets of  $\ln (H_v^{-3} - H_{v0}^{-3})$  values at different temperatures were obtained for three different values of  $\ln (t^{1/3} - t_0^{1/3})$  indicated by vertical broken lines. These values of  $\ln (H_v^{-3} - H_{v0}^{-3})$  were plotted against the inverse of corresponding temperature. Again these curves are straight lines with approximately equal slopes according to equation. (5) The slope represents the value of  $Q/3R$ . The activation energy thus obtained is listed in Table – 3.

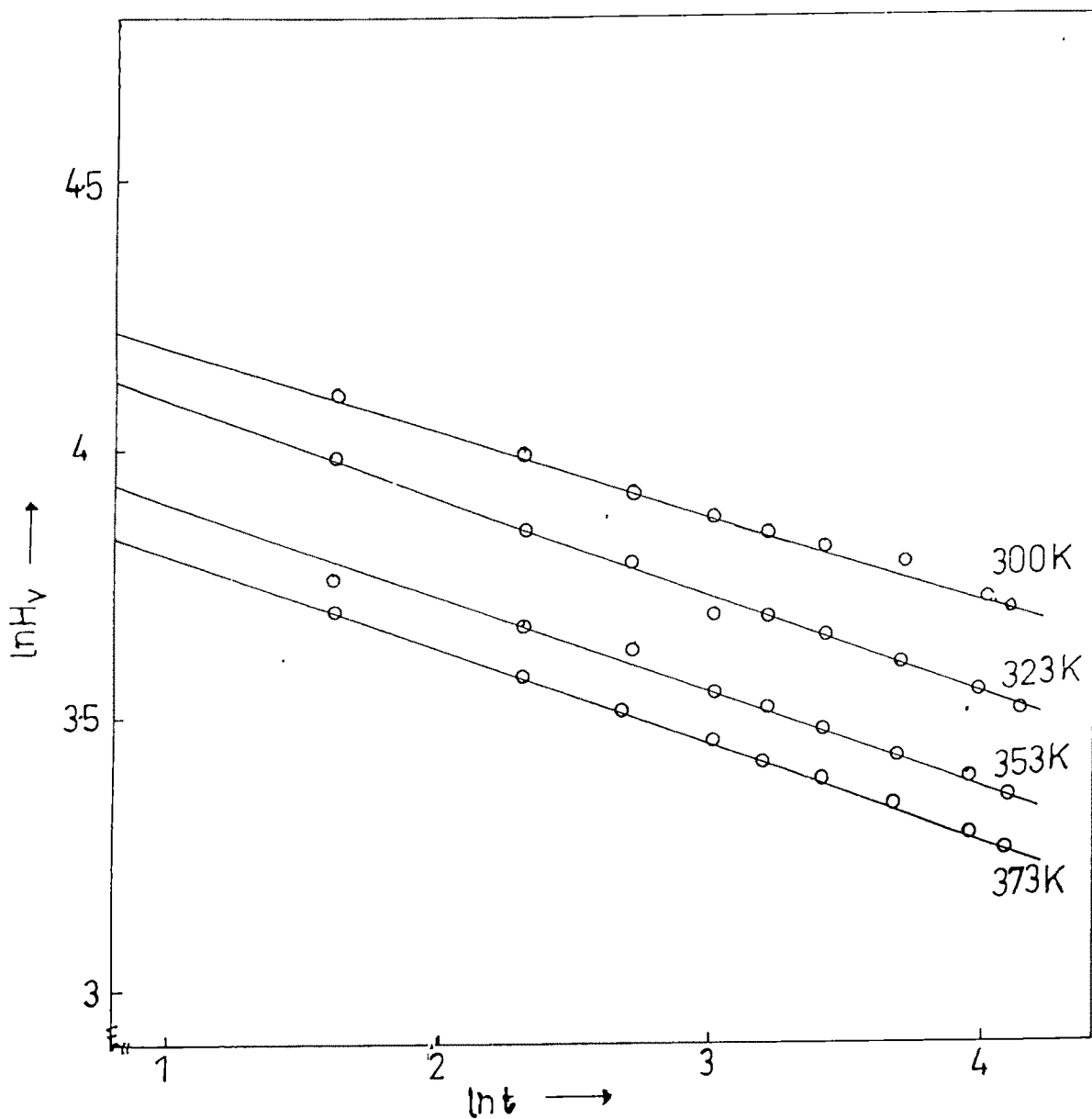


Fig.12. Plots of  $\ln H_v$  versus  $\ln t$  for  $\text{In}_{0.1}\text{Bi}_{1.9}\text{Te}_3$  crystals.

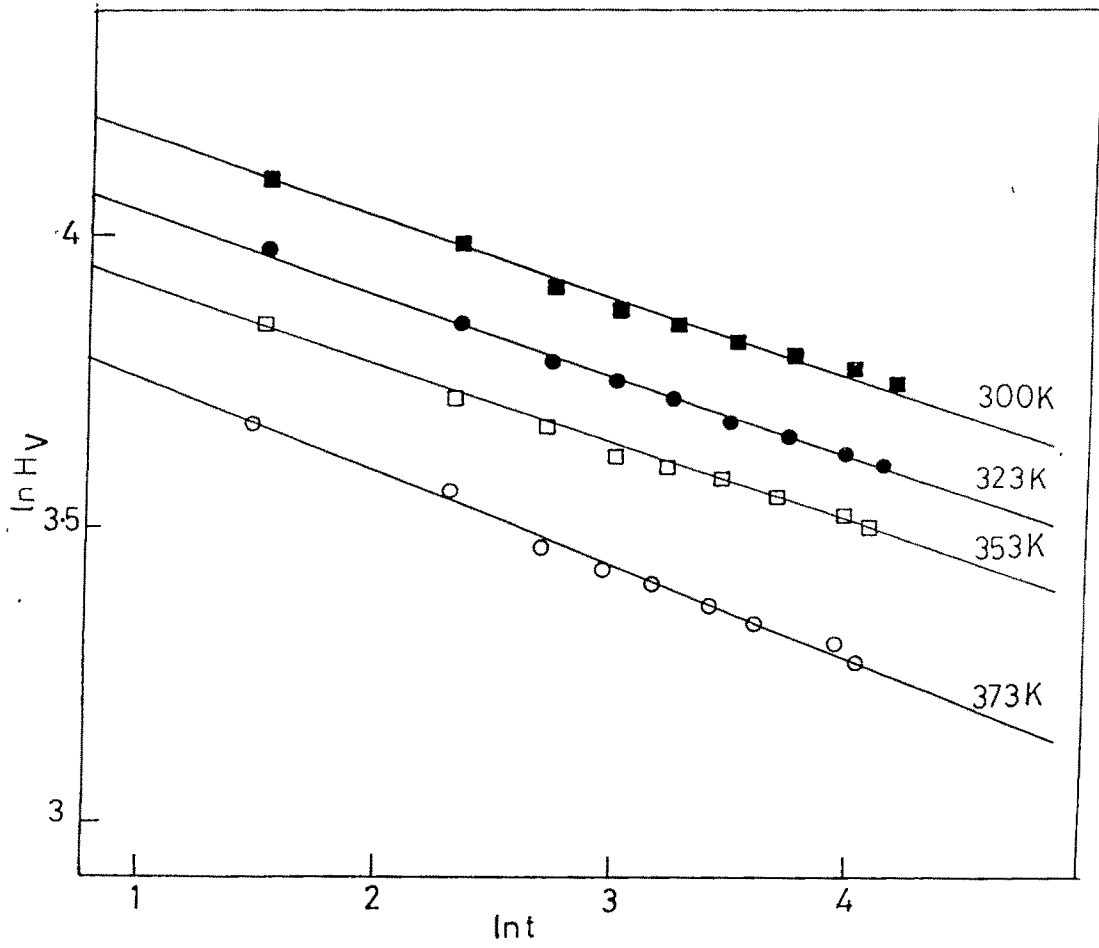


Fig.13. Plots of  $\ln H_v$  versus  $\ln t$  for  $\text{In}_{0.2}\text{Bi}_{1.8}\text{Te}_3$  crystals.

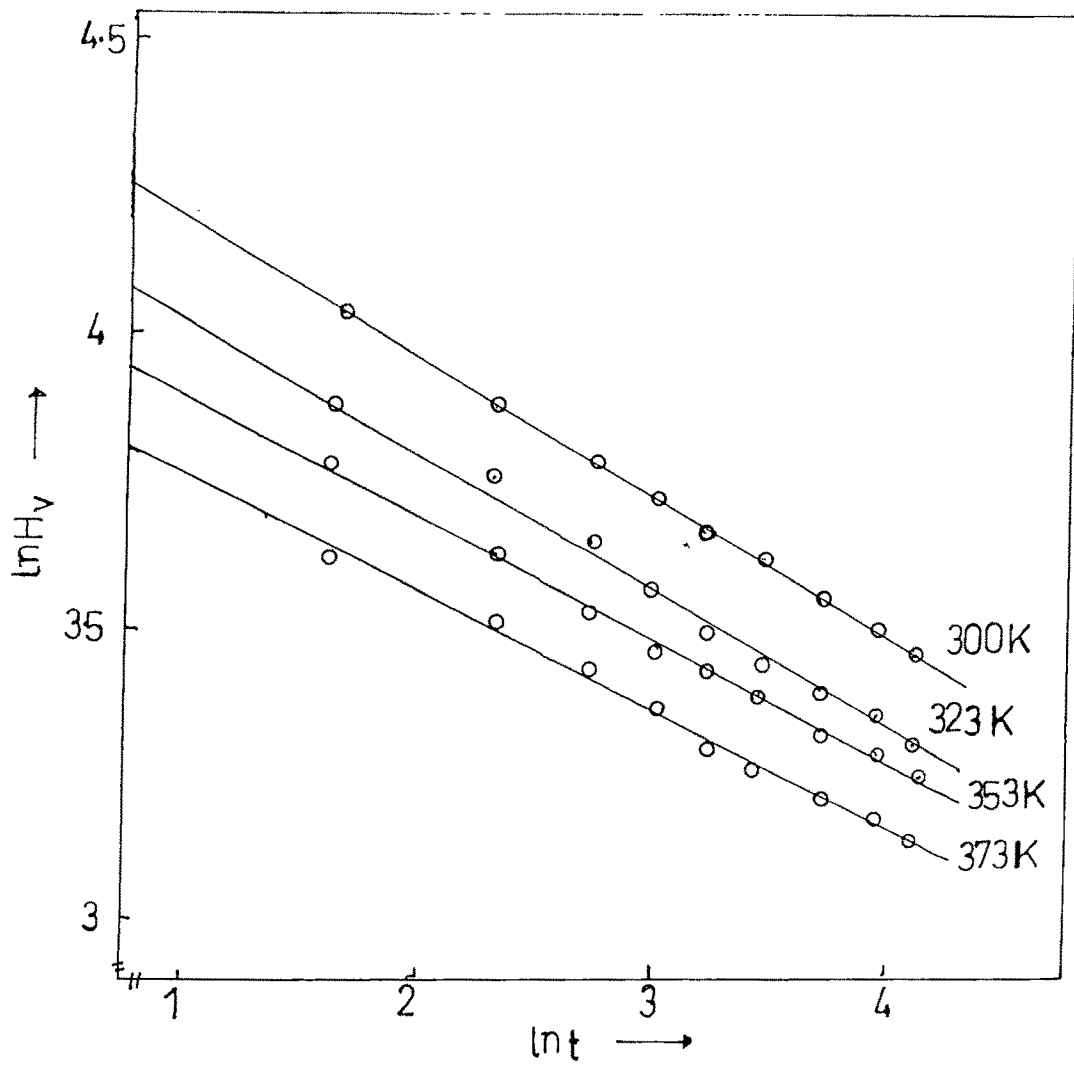


Fig.14. Plots of  $\ln H_v$  versus  $\ln t$  for  $\text{In}_{0.5}\text{Bi}_{1.5}\text{Te}_3$  crystals.

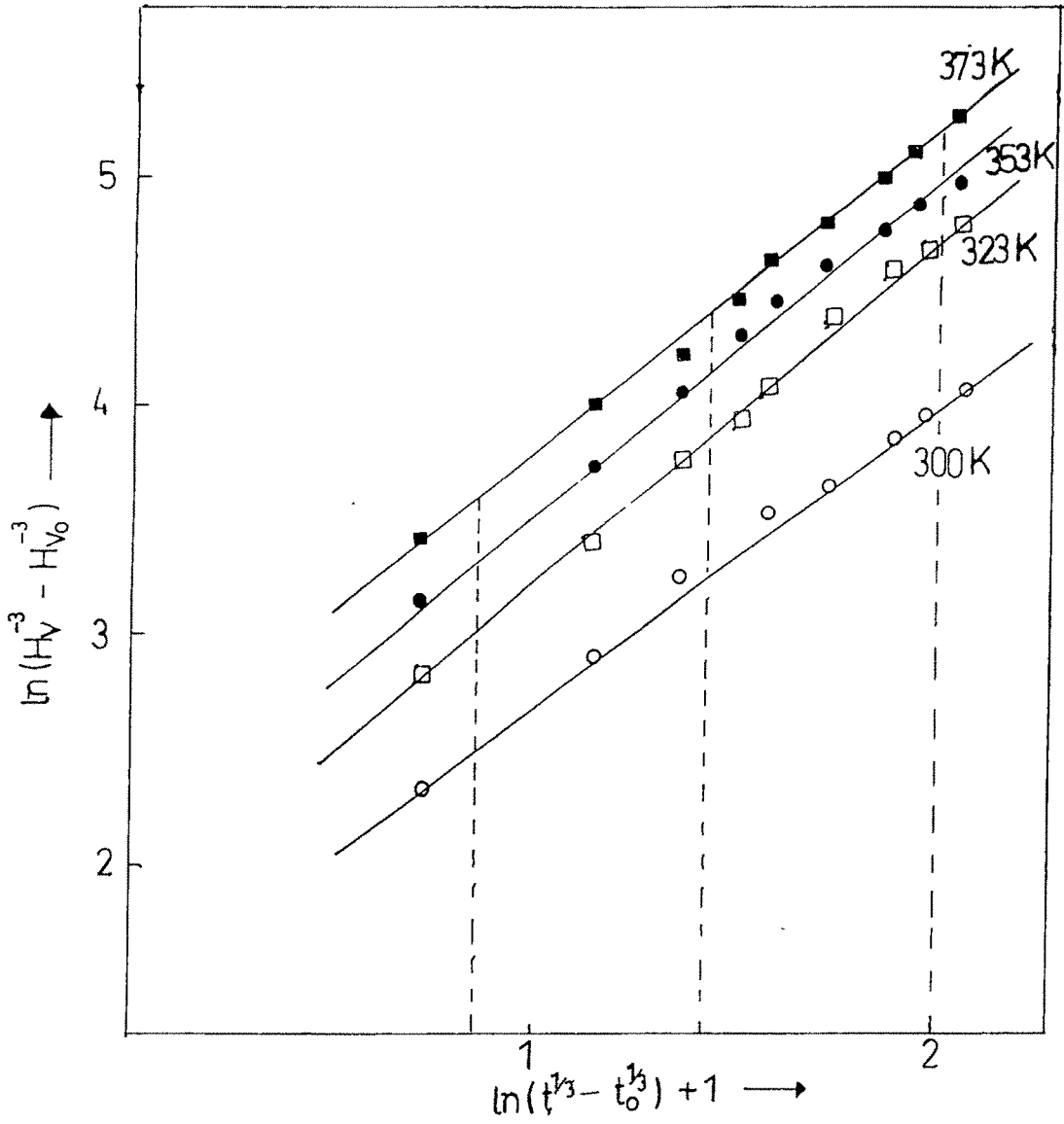


Fig.15. Plots of  $\ln(H_v^{-3} - H_{v_0}^{-3})$  versus  $\ln(t^{1/3} - t_0^{1/3})$  for  $\text{In}_{0.1}\text{Bi}_{1.9}\text{Te}_3$  crystals.

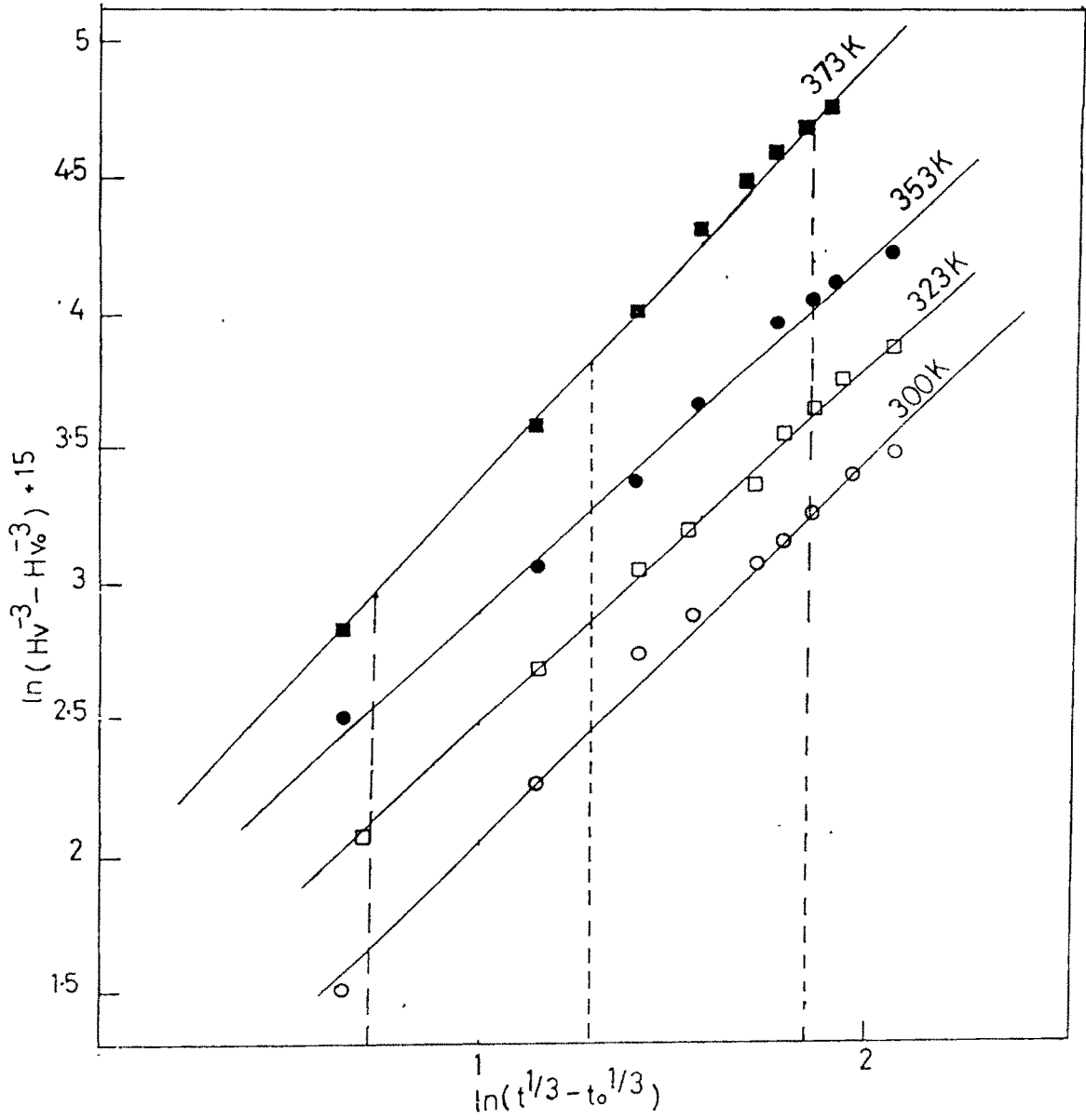


Fig.16. Plots of  $\ln (H_v^{-3} - H_{v_0}^{-3})$  versus  $\ln (t^{1/3} - t_0^{1/3})$  for  $\text{In}_{0.2}\text{Bi}_{1.8}\text{Te}_3$  crystals.

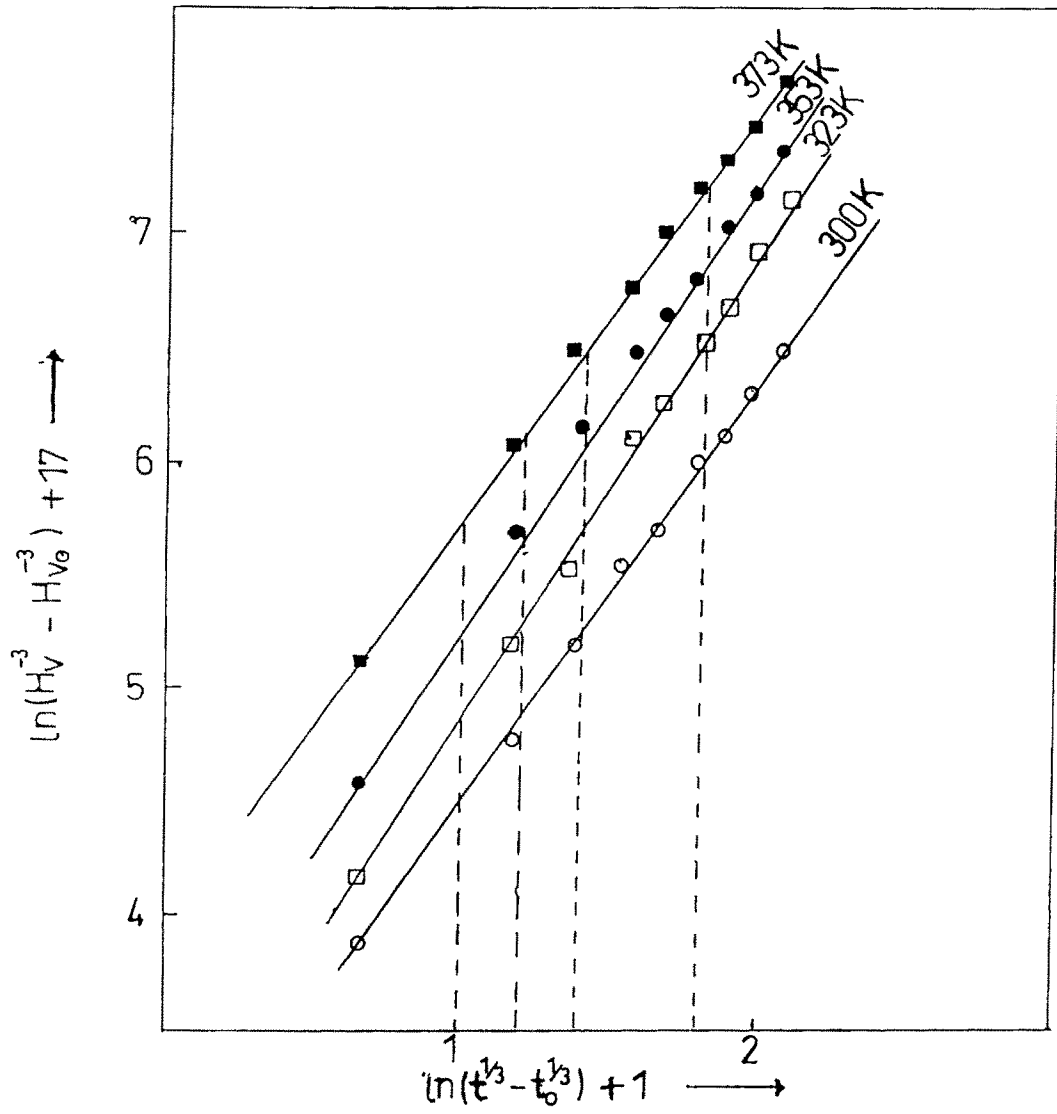


Fig.17. Plots of  $\ln (H_v^{-3} - H_{v_0}^{-3})$  versus  $\ln (t^{1/3} - t_0^{1/3})$  for  $\text{In}_{0.5}\text{Bi}_{1.5}\text{Te}_3$  crystals.

**Table -3**

x of In in $\text{In}_x\text{Bi}_{2-x}\text{Te}_3$	Activation energy Kcal/mole
0.1	12.1
0.2	13.6
0.5	18.1

## CONCLUSION :-

- 1) The hardness values of  $\text{In}_{0.1}\text{Bi}_{1.9}\text{Te}_3$ ,  $\text{In}_{0.2}\text{Bi}_{1.8}\text{Te}_3$  and  $\text{In}_{0.5}\text{Bi}_{1.5}\text{Te}_3$  single crystals have been obtained to be 30.6, 36.2 and 49  $\text{kg/mm}^2$  respectively which are significantly higher than the reported hardness of the pure  $\text{Bi}_2\text{Te}_3$  crystals.
- 2) Microhardness is load dependent quantity and the variation is quite prominent in the low load range and for high applied loads it becomes virtually independent of load.
- 3) Due to work hardening, the crystal hardness increases. The Meyer index is not truly constant but may be different in different load ranges.
- 4) The work hardening capacity of  $\text{In}_{0.5}\text{Bi}_{1.5}\text{Te}_3$  crystals has been observed to be the highest among the three crystals.
- 5) The surface anisotropic variation of hardness is consistent with the six fold axis of symmetry.
- 6) The creep study indicates that as indium concentration increases the temperature softening parameter increases and also creep activation energy increases.

## REFERENCES :

1. Tabor. D., The Hardness of metals (oxford Univ.) (1951).
2. Bergsman, E.B., Met. Progr., 54 (1948) 153.
3. Rostoker. W.J., Inst. Met., 77 (1950) 1975.
4. Grodzinsky, P., Indust. Diam Rev., 12(1952) 209, 236.
5. Taylor, E.W., J. Inst. Met., 74 (1948) 493.
6. Toman, I.Jr., Nye, W.F. and Gelas, A.J., 5<sup>th</sup> Inst. Cong. Electron Microscopy, I(1962) FF.13.
7. Onitsch, E.M., Schweiz Arch, angew Wiss 19 (1953) 320.
8. Buckel, H., Med. Rev., 4(1959) 49.
9. Bochaver A.A., and Zhardaeva O.S., Bull. Acad. Sci., URSS, 3 (1947) 341.
10. Onitsch E.M., Mikroskopie, 2(1947) 131.
11. Buckle. H., Rev. Metall, 48 (1951) 957.
12. Braunovic, The Sci., of hardness Testing and its Research applications eds. By Westbrook and Conrad H., (ASM, Ohio), (1973) 329.
13. Mott. B.W. Micro hardnemindeintation testing (butter wort's pub.) London (1956).
14. Atkins, A.G.Silverio. A., and Tabor D., J. Inst. Metals 94 (1966) 369.
15. Ito K., sci papers Sandai, Tohoku Univ., Ser. 1.(1923) 137.
16. Shiskokin V.P. Z. Anorg. Chem., 189 (1963) 263.

17. Hargreaves F., J. Inst. Metals, 39 (2928) 742
18. Mott N.F., Phil. Mag. 44 (1953) 742.
19. Fujiwara M. and Hirokawa T., J. Jap. Inst. Metal. (Japan), 56, 2 (1992).
20. Sgobba, B. Geibel, W. Blum, Phys. Stat. Solidi (a) 137, 2 (1933) 363 – 79.
21. Ayensu, G.K. Guainoo, S.K. Adijeponag, J. Mat. Sci. Lett. (UK), 12, 13 (1993) 1008 –10.
22. Shah R.C. Ph.D., Thesis, M.S. Univ. of Baroda (1984).
23. Bhatt V.P., and Desai D.F., Bull. Mater. Sci, 4, 1 (1982) 23-28.
24. Trivedi M.D., Ph.D. Thesis, M.S. Univ. of Baroda (1944).
25. Jain T.M., Ph.D. Thesis, M.S. Univ. of Baroda (1995).
26. Desai C.F., Soni P.H. and Bhavsar S.R. bull Mater Sci., Vol. 22, 1 (1999) 21 – 23.